DIRECT DOWN CONVERSION RECEIVERS AND INTERMODULATION BALANCE

Masters Thesis

RYAN CLEMENT
43593917

Table of Contents

Table of Figures

1. Abstract

Direct down converting receiver architecture is reviewed. The impetus for moving towards this architecture is driven by cost, however it does have some design drawbacks. Volterra analysis is used to show how coefficients often neglected in heterodyne radios can play a significant part in the overall performance of a radio, although careful review of any spurious tones should be analysed before switching to this design topology. Measurements are taken with different devices from two process technologies - Gallium Arsenide (GaAs) and Silicon Germanium (SiGe) with differing results. Overall the GaAs devices are more linear, however the second order performance is significantly better with SiGe and it is thought that this could be attributed to balance.

2. Introduction

Direct down conversion receivers is a topic that isn't entirely new. It was first mentioned back in 1924[1]. The revived interest in the topic is primarily driven by cost, however there are numerous issues that must be addressed before committing to such an approach, which is why heterodyne receivers have been the mainstay of radio design for almost eighty years [2].

The homodyne receiver can also be referred to as a zero Intermediate Frequency (IF) receiver, i.e. it is able to go directly from the baseband signal to the final Radio Frequency (RF) stage, eliminating any intermediate mixing stages in the RF chain. The ability to reduce the components in a radio is advantageous for both reliability and cost, and technical reasons, such as the removal of the image frequency and the availability of baseband amplifiers, also play into the hand of homodyne radios. To improve the output from the baseband signals, low pass filters can be easily implemented, are cost effective and generally simpler to build than the equivalent-performing band pass filters associated with heterodyne systems. In fact, often the biggest advantage of a homodyne radio is also its biggest disadvantage, and that is that the Local Oscillator (LO) frequency is the centre carrier frequency. This LO is normally quite strong and if sufficient suppression isn't in place, it will cause issues at the antenna, producing interference for other systems in addition to itself if reflected or coupled internally. If the system can reduce the leaked LO power to sufficiently low levels, other intermodulation (IM) products normally unimportant in heterodyne based designs can cause issues. Even order products (2xLO-2xRF for example) may fall into the baseband output and are difficult to eliminate. Other problems include the generation of DC

offsets [3] and flicker noise, which add further complexity in dealing with overall performance of the system. Flicker noise will be discussed briefly in Section 2.1 to provide an overview of the complexity of this problem, as it is a driving issue hampering the implementation of direct conversion receivers.

The differences between heterodyne and homodyne intermodulation are explored, highlighting some of the challenges with direct down conversion radios. Comparisons are made between receivers using different processes followed by a discussion of how balance within the chip can alter the intermodulation performance.

2.1 Flicker Noise

Many architectures for homodyne down converting mixers have been evaluated in published literature. Rubiola [4] provides a detailed tutorial into double balanced mixers, including details of operating modes for these types of mixers and their uses in different scenarios such as with phase detectors. The tutorial demonstrates when mixers should be run into saturation and highlights the benefits of image reject mixers. Rubiola analyses noise and notes that these mixers are generally specified for white noise performance. Flicker noise in mixers is often not evaluated purely for flicker noise performance, but more as a means for measuring the phase noise performance of oscillators [4]. There is an expectation that the LO side of the mixer is the main source of introducing flicker noise to the output of the mixer, but it is yet to be proven as an absolute [4]. However there is no mention of whether an image reject mixer is still a useful component to have in a homodyne system when there is no image present but perhaps there are benefits with improved noise figure that still apply.

Flicker noise is a concept that is found in a wide variety of fields and is not limited to the world of electronics, showing up in studies of ocean currents [5], audio signals [5] and population growth [6]. The presence of flicker noise in electronics was initially discovered by Johnson in 1925 [7] while looking for shot noise [5]. During the almost ninety years from that discovery there have been numerous theories and measurements to understand the basis of this noise and how to minimise its influence (a summary of theories is listed in [8, 9]). Flicker noise can be defined in a number of different ways and referred to by a number of terms, such as flicker, *1/f* and pink noise. Flicker noise contains an equal amount of noise power in each sequential octave which equates to having a slope of 10 dB per decade, although it has been reported that this slope can be variable and it is closer to $1/f^{\alpha}$ where α is somewhere been 0.5~1.5 [5]. White noise the most commonly known noise, being present everywhere, with a constant power density and a mean value of zero. If there were no other influences in a system, the only noise generated would be white noise, which consists of electron vibrations. This was presented by Johnson in 1928 [10]. The formula for this thermal noise is defined by:

$$P=kTB \tag{1}$$

(where k = Boltzmann's constant, T is temperature in kelvin and B is the bandwidth of the device).

It is notable that this formula is independent of resistance, so the thermal noise power available from a 1 Ω resistor is the same as that delivered from a 1 MΩ resistor. At 290 K the minimum theoretical noise is therefore -174 dBm/Hz, and hence the only way to eliminate thermal noise completely would be to operate the device at absolute zero

(something that is not yet achievable nor would be practical in a commercial sense). The intersection point between flicker noise and white noise is referred to as the corner frequency (f_c)[8]. The measured value at the corner frequency is 3 dB higher than the white noise value due to the summing of the two powers (see Figure 1). White noise is defined as an additive noise, in that it adds a constant amount of power to both amplitude and phase noise [11] (an example showing how white noise can affect both the amplitude and phase of a signal is shown in Figure 2 [8]). Flicker noise (and higher order $1/f^{\alpha}$ noise) can be regarded as multiplicative noise source, as it is not correlated and can be converted in differing amounts with respect to amplitude and phase [11].

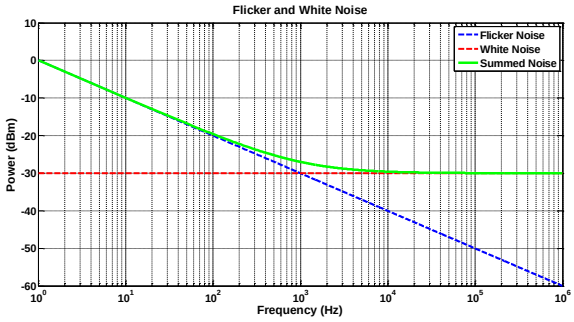

Figure 1 - Noise Power

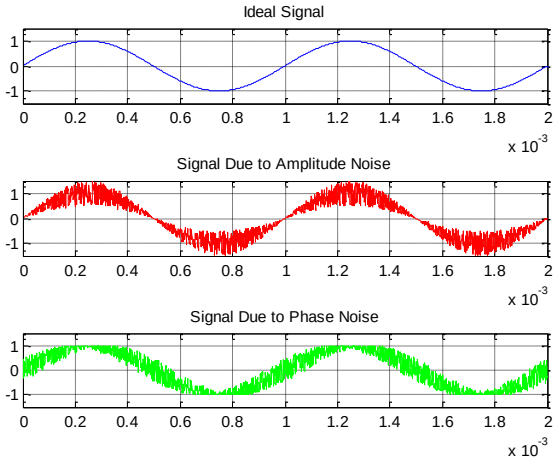

Figure 2 - Amplitude and Phase Noise

The significance of the corner frequency is that it provides the user with the minimum point where the device can be operated, ensuring the lowest possible noise figure for the whole system. For instance in a heterodyne-based radio, having the IF above the corner frequency reduces the noise at the IF output and hence improves the overall performance. This scenario changes with a homodyne system especially if the bandwidth of the modulated signal is smaller than the corner frequency. For instance if f_c=10 kHz and the baseband bandwidth was 56 MHz, the overall noise impact would likely be minimal from the 0.02% of the channel. However an f_c=1 MHz with a channel of 500 kHz would significantly degrade the overall signal-to-noise ratio and thus limit the use of the radio.

GaAs pseudomorphic High-Electron-Mobility Transistor (pHEMT) technology has been shown to provide the lowest noise out of GaAs technologies such as Metal-Semiconductor Field-Effect Transistors (MESFETs) and Heterojunction Bipolar Transistors (HBTs) [12]. The flicker noise within GaAs Monolithic Microwave Integrated Circuits (MMIC) is regarded as being worse than that of Silicon-based technologies [9], however Campbell *et al.*[13] and Huang *et al.* [14] have shown, at least with MESFET and pHEMT based devices, that flicker noise can be minimised with very low drain-source voltages. Manstretta *et al.* [15] have demonstrated that within CMOS devices, very low drain voltages (minimising voltage noise) will optimise the noise power that is generated within a mixer. Further CMOS work has been completed demonstrating (with a Gilbert cell mixer) that the addition of resonating inductors can further reduce flicker noise when designing mixers[16]. All reported work did show that flicker noise can be

reduced for a discrete mixer, but it didn't report the impact of this performance on linearity, gain, frequency spurs and thus overall performance in a larger system.

In order to measure flicker noise, a Low Noise Amplifier (LNA) is required to boost the power before measurement by a spectrum analyser. Commercially available LNAs designed for measuring flicker noise often are not matched for 50 Ω measurements and the apparent noise figure increases when operated at the source impedance of 50 Ω (see Figure 3).

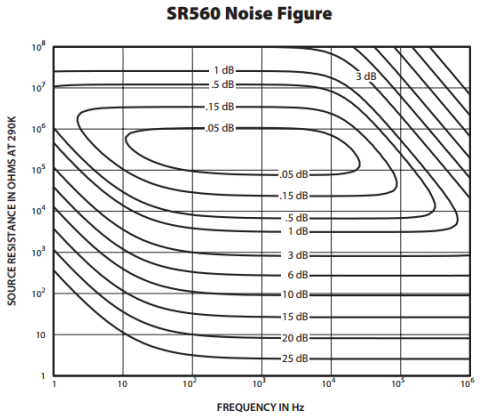

Figure 3 - SR560 Noise Figure vs Source Resistance [17]

This causes difficulties when differentiating between the Device Under Test (DUT) noise figure and LNA noise figure. Rubiola *et al.* [18] have designed and built a 50 Ω matched LNA specifically for noise measurements. This reference design has been utilised elsewhere [19, 20] providing confidence that it can be replicated. The final issue is that a calibrated noise source below 10 MHz has been difficult to obtain. As a result the thermal noise from a 50 Ω resistor is used (sometimes over large temperature ranges) which, as mentioned previously is -174 dBm/Hz, and cascaded gain is worked backwards from spectrum analyser data to work out the noise being generated in the DUT [18, 21].

This technique relies on no external interference and should be completed in a screened area for accurate measurements.

3. Intermodulation within Downconverters

Higher levels of integration in system designs means that tighter intermodulation specifications are required [22]. It is now common to find MMICs that contain LNAs with mixers and LO multiplier stages on a single device. While this is extremely attractive to a system designer it adds considerably to the design of the MMIC, places pressure on the chip designer to meet tighter specifications and adds a layer of complexity to debugging a design. The addition of the LNA with the mixer results in a secondary source of distortion that is applied to the mixing stage and hence one considers not only the two wanted tones but any other tones that happen to fall in the pass band of the LNA. At a minimum this would be two additional third-order intermodulation (IM3) signals, combining for a total of four signals (two wanted and two subtractive IM3 terms) which can then further mix with each other and add to the "congestion" at base band. Subtractive tones are defined as tones that are generated by the difference between two signals rather than the addition of tones (additive tones). In later chapters additive and subtractive tones will be explored further.

The second source of interfering signals is from the LO chain. The best performance is obtained with a clean Dielectric Resonator Oscillator (DRO) at the frequency of operation. However, this is usually not a cost effective option, so cheaper, and subsequently noisier solutions are required. If the DUT has an LO stage that consists of frequency multiplication and amplification, then further sources of mixing can occur.

Intermodulation is the creation of spurious products by non linearities. In many industries, and in particular telecommunications, this is a key measure for designing

amplifiers and mixers in order to create a system that can operate effectively over a large dynamic range. The introduction of direct down conversion receivers can be strongly influenced by higher order non linearities therefore particular attention must be paid during the system design process.

In designing a communication system, it is useful to calculate how significant the intermodulation distortion will be as this will determine the performance of the overall system. Before further consideration of the two tone case, it is prudent to explain why two tones provide such insight into an environment that will rarely have two signals on it. Two tone testing is a simple, repeatable and industry-accepted method for comparing devices. It does not look to have optimised algorithms that can exploit particular characteristics of the semiconductor, such as digital pre distortion, but merely tries to evaluate the analogue performance of a device excited with two equal-power, closely-separated tones and establishes a theoretical point whereby the nth order intermodulation tone would intersect with the projected level of a monotonically increase tone.

The real world scenario will require the radio to have a complex signal, that is, the payload does not consist of two distinct sine waves (an example of a baseband data payload for 16QAM (Quadrature Amplitude Modulation) is shown in Figure 4). This data could be modulated in a number of ways such as Phase-Shift Keying (PSK) or QAM architectures. These complex signals occupy bandwidth determined by the resulting symbol rate and the effect of the pulse shaping or filtering that is applied. A raw unfiltered spectrum is shown below in Figure 4 and Figure 5.

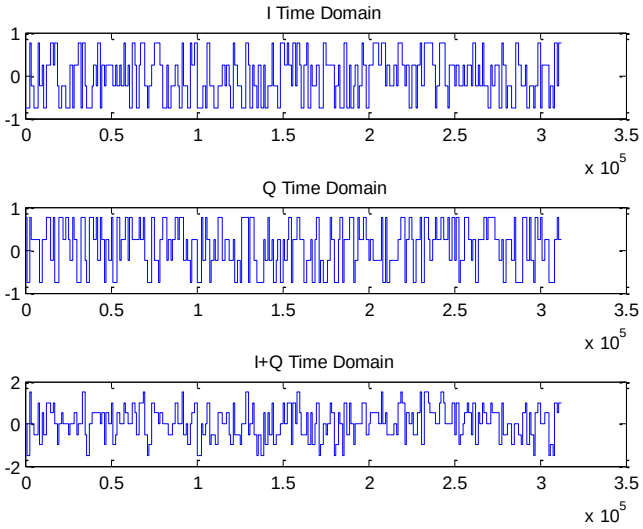

Figure 4 - 16-QAM data payload

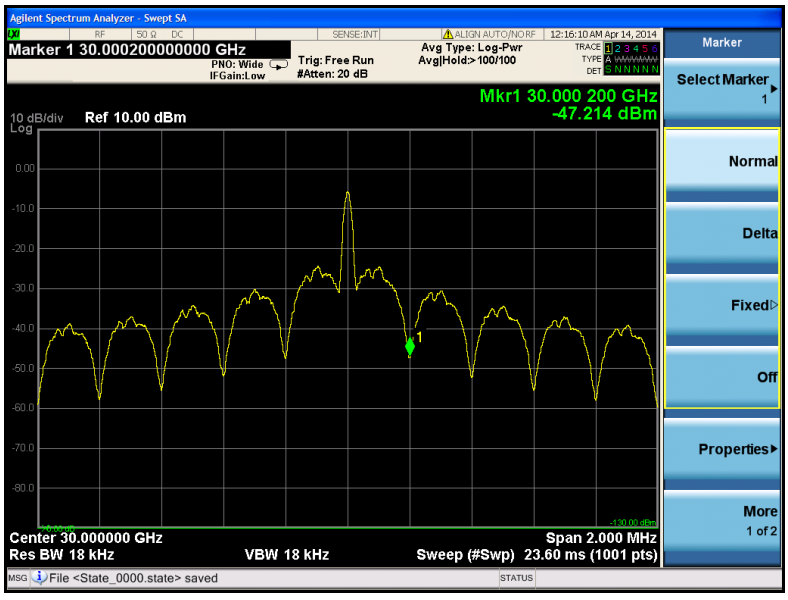

Figure 5 - Modulated 16-QAM signal with unfiltered I and Q baseband signals and significant LO breakthrough

Once the device enters non-linear operation, additional care is required as large signal-interfering products are generated within the device itself, introducing distortion and hence bit errors into the signal. When modelling in the small signal region, Taylor series-based models can be used. Once the device is driven into non-linear regions, alternative models are required to simulate these intermodulation tones [23].

The intermodulation terms themselves are measured simply as a power level but can often be referred to as the carrier tone known as Carrier to Interferer (C/I) or secondly as an intermodulation intercept point. This intercept point ties the interferer tone to the carrier signal and refers it to the input or the output of the DUT. As discussed, this point is a theoretical point whereby the intermodulation tone power would equal (or intercept) the carrier tone power. In reality this point can never be met but is used as an order of merit for evaluating the performance of a system. Calculating the intercept point is calculated by the following formula: [24]

$$\mathrm{IIP_n} = \mathrm{P_i} + \frac{\mathrm{P_o} - \mathrm{P_{IMn}}}{\mathrm{n}-1} \qquad (2)$$

and referred to the output

$$\mathrm{OIP_n} = \mathrm{P_o} + \frac{\mathrm{P_o} - \mathrm{P_{IMn}}}{\mathrm{n}-1} \qquad (3)$$

(where $IIP_n, OIP_n,\ P_i,\ P_o$ & P_{IMn} are all in dBm)

The measure of IP_n typically gives insight into how well a device can resolve two signals. The lower the IP_n result the larger the intermodulation signals become and hence the more distorted the output appears.

4. Intermodulation with respect to amplifiers

Intermodulation is a general term and can be made up of an infinite number of components, however most are so small they have negligible effect on the output of the device (and measuring beyond the seventh order is difficult due to terms falling below the noise floor of spectrum analyser which is typically -100 dBm depending on resolution bandwidth). It is generally accepted that the key terms that can cause issues with system performance are third order terms, and in particular for amplifiers, the subtractive $2f_1 - f_2$ and $2f_2 - f_1$ terms. The reason for this is that they generally fall in the same band as the wanted signal, passing uninhibited through the system, and the third order terms also typically have enough power to cause system issues. For example, consider two tones: 38.041 GHz and 38.053 GHz. If the device had an operating range from 37 to 40 GHz, the second order tone 2 x 38.041 = 76.082 GHz would be outside the operating range of the device and hence wouldn't interfere with subsequent components in the chain. However, 2 x 38.041-38.053 = 38.029 GHz would fall in band and would pass through to the remaining system, potentially causing signal interference and potentially distortion in the amplifier if the increased output power causes compression. The tone would be too close to the main carrier to filter in conventional sense so achieving linearity sufficient to suppress these tones is of high importance.

Being able to describe the linearity of device is useful for numerous reasons, such as comparing similar devices, but also for predicting how a device will perform in a system. In an ideal, linear system, an increase in power will directly translate into a constant increase of power at the output of the system. In an ideal world this would continue to

infinity or the next best thing - immediately hit saturation. However due to physical limitations there are numerous other distortion signals that limit this from occurring. Many of these interferer tones are below the noise floor at small signal power levels, but appear as power levels increase.

Intermodulation can be measured by injecting two tones and measuring the mixing elements. Consider an input signal of two tones:

$$V_i = Acos(\omega_1 t) + Acos(\omega_2 t) \quad (4)$$

The output through a nonlinear device can be represented as a Taylor series in the linear region.

$$\mathrm{V_o} = \mathrm{k_1 V_i} + \mathrm{k_2 V_i^2} + \mathrm{k_3 V_i^3} + \cdots \quad (5)$$

Substituting $V_i$into V_o :

$$V_o = A^2k_2 + \frac{1}{4}(4Ak_1 + 9A^3k_3)cos[\omega_1 t] + \frac{1}{2}A^2k_2cos[2\omega_1 t] + \frac{1}{4}A^3k_3cos[3\omega_1 t] + \frac{1}{4}(4Ak_1 + 9A^3k_3)cos[\omega_2 t] + \frac{1}{2}A^2k_2cos[2\omega_2 t] + \frac{1}{4}A^3k_3cos[3\omega_2 t] + \frac{3}{4}A^3k_3cos[\omega_1 t - 2\omega_2 t] + A^2k_2cos[\omega_1 t - \omega_2 t] + \frac{3}{4}A^3k_3cos[2\omega_1 t - \omega_2 t] + A^2k_2cos[\omega_1 t + \omega_2 t] + \frac{3}{4}A^3k_3cos[2\omega_1 t + \omega_2 t] + \frac{3}{4}A^3k_3\, cos[\omega_1 t + 2\omega_2 t] + \cdots \quad (6)$$

In the case of an amplifier most of the terms are outside the pass band of the amplifier and so are negligible, however the subtractive 3rd order terms can fall in the amplifier band and can cause problems. The coefficients theoretically go to infinity, but the higher order terms are so small they can be neglected. The k_1 term is normally associated with the bulk of the gain of the device, as in a perfect system there would be no intermodulation and all other coefficients would be zero, leaving Ak_1.

5. Intermodulation with respect to balanced amplifiers and mixers

Reasons for considering balance in a system include better noise resilience, and that double the power can be transported over similar line width. The basis of a balanced system is to have two signals separated by 180° that are then combined at the end of the system. The motivation for balance, when analysing intermodulation, is that the even order products cancel leaving only the odd order products. Let V_1 be the original two tone signal. If we take another signal that is offset 180°, V_2 is generated which can be simplified as $-V_1$.

$$V_1 = Acos(\omega_1 t) + Acos(\omega_2 t) \quad (7)$$

$$V_2 = Acos(\omega_1 t + \pi) + Acos(\omega_2 t + \pi) \quad (8)$$

$$V_2 = -Acos(\omega_1 t) - Acos(\omega_2 t) \quad (9)$$

$$V_{o1} = k_1 V_1 + k_2 V_1^2 + k_3 V_1^3 + \cdots \quad (10)$$

$$V_{o2} = k_1 V_2 + k_2 V_2^2 + k_3 V_2^3 + \cdots \quad (11)$$

Limiting expansion to the third order expression

$$V_o = V_{o1} - V_{o2} \quad (12)$$

$$V_o = \frac{1}{2}(4Ak_1 + 9A^3k_3)cos[\omega_1 t] + \frac{1}{2}A^3k_3cos[3\omega_1 t] + \frac{1}{2}(4Ak_1 + 9A^3k_3)cos[\omega_2 t] + \frac{1}{2}A^3k_3cos[3\omega_2 t] + \frac{3}{2}A^3k_3cos[\omega_1 t - 2\omega_2 t] + \frac{3}{2}A^3k_3cos[2\omega_1 t - \omega_2 t] + \frac{3}{2}A^3k_3\,cos[\omega_1 t + 2\omega_2 t] \quad (13)$$

In an amplifier where the even order products are out of band this balance does not confer many benefits with respect to linearity however; when evaluating mixers where the difference between the two signals is the goal, this balance can be a useful technique to eliminate unwanted interference (Figure 7). This balance is utilised in mixers that have a differential output.

If there is any phase or amplitude imbalance in the system, the even order terms will again be present but at a smaller magnitude. Assuming an amplitude imbalance α and phase imbalance of θ the output voltage will look like the equation below.

$$V_o = 2Ak_2\alpha - k_2\alpha^2 + \left(Ak_1 + \frac{9A^3k_3}{4}\right)cos[\omega_1 t] + \left(Ak_1 + \frac{9A^3k_3}{4} - k_1\alpha - \frac{27}{4}A^2k_3\alpha + \frac{27}{4}Ak_3\alpha^2 - \frac{9k_3\alpha^3}{4}\right)cos[\omega_1 t - \theta] + \frac{1}{2}A^2k_2cos[2\omega_1 t] + \left(-\frac{A^2k_2}{2} + Ak_2\alpha + \frac{k_2\alpha^2}{2}\right)cos[2\omega_1 t - 2\theta] + \cdots \quad (14)$$

From these equations it can be seen that for every dB of input power the IM2 terms will increase at two times the rate, and the IM3 terms will increase at three times the rate of the input signal (Figure 6). This trend continues for higher order products. While this is the commonly accepted view of intermodulation (and to a large extent this is observed in most devices) there are cases where this general expansion doesn't quite track real physical measurements. There could be a number of reasons for this but notably Cripps [25] points out that depending on the coefficients that a polynomial expansion provides, there are points where nulls or cancellation can occur. For instance, if one assumes that the only significant coefficients that will contribute to the output signal are odd such that

$$V_{o1} = k_1V_1 + k_3V_1^3 + k_7V_1^7 + \cdots \quad (15)$$

it is possible to get third order terms that can cancel

$$V_{IM3} = \frac{3A^3k_3}{4} + \frac{735A^7k_7}{64} + \cdots \quad (16)$$

From this equation it can be seen that if k_3 & k_7 have opposite signs, a null point is possible, and that the straight line below (Figure 6) may not be quite what it is initially predicted to be.

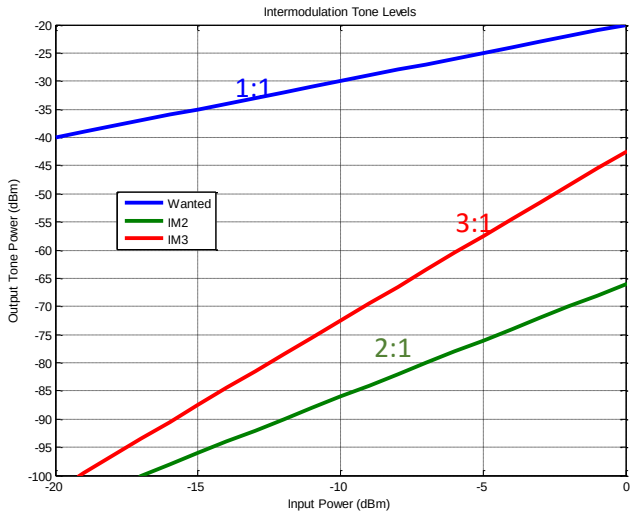

Figure 6 - Intermodulation Tone Levels

It can also be seen from the IM2 terms that the power will have a dominant $1 - \cos(2\theta)$ with subsequent higher order terms.

$$\frac{A^2 k_2}{2}(1 - \cos(2\theta)) + \frac{45A^4 k_4}{8}\left(1 - \frac{36}{45}\cos(2\theta) - \frac{9}{45}\cos(4\theta)\right) \text{ when } t = 0 \qquad (17)$$

Ignoring these higher order terms leads to the following relationship which must be also considered when comparing devices i.e. the imbalance of the system will also lead to increased intermodulation power. As shown below (Figure 7), with 0 degrees of imbalance the IM2 tones will completely cancel as shown by the null. In this particular scenario the two signals have been assumed to have the same amplitude. It is quite

plausible that the 0 and 180 degree branches have different amplitudes which would change this relationship.

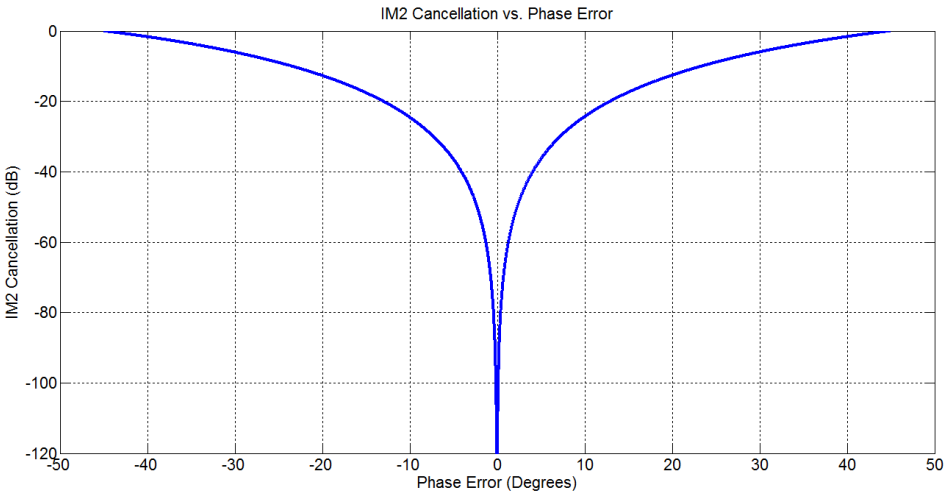

Figure 7 - IM2 Cancellation

In this homodyne scenario the presence of these intermodulation terms will pay a significant price in the overall performance of the system. This is due to a number of terms falling into the baseband spectrum. For instance, consider again two tones 38.041 GHz and 38.053 GHz that are mixed with a local oscillator of 38 GHz. In a direct down conversion mixer, the wanted tones would be 41 MHz and 53 MHz, whereas the unwanted tones up to the seventh order will be present out to and beyond 160 MHz. Figure 8 shown below is a graph displaying both the additive and subtractive tones out to 160 MHz and plotting orders one through to seven. While a seventh order tone will increase at a rate of 7:1 compared to the input tone, the reality is, higher order tones tend to be of a lower power when the DUT is backed off from the saturation point. Therefore in order to measure higher order terms significant input power may be required to get above the noise floor of the spectrum analyser, however this may mean distortion may already be occurring for these higher order tones before it is possible to measure them with the laboratory equipment.

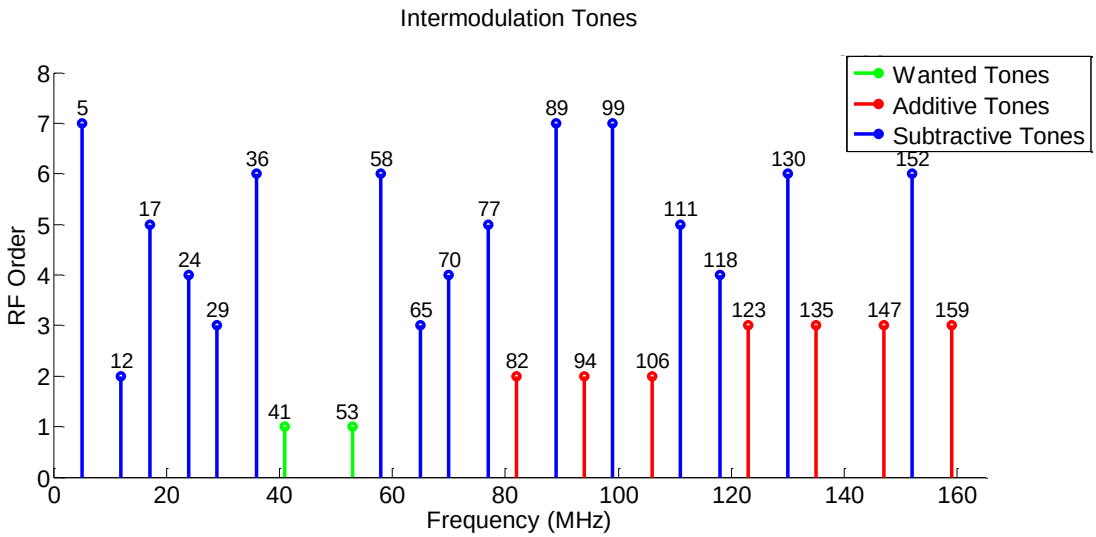

Figure 8 - Intermodulation Tones

Additive terms are defined as terms that mix two positive terms i.e. n*f1+m*f2 (each term has same sign), whereas subtractive terms are $\pm$n*f1$\mp$m*f2 (that is each term has opposite sign). The second order products also contribute to the DC offset as shown above. This can be critical for the Analog to Digital Converter (ADC) in detecting the correct signal without it hitting the rail of the device and causing demodulation errors.

Therefore, when considering the performance of a single chip downconverter, characterisation of the intermodulation performance needs to take into account not only the traditional two tone IM3 levels, but all intermodulation tones from each successive element. In the case we are describing with LNA and mixer, it will make it essentially making it a effectively a four tone IP3 measurement (assuming the third order tones are the only other significantly powerful tones). The equations below show that the amplitude of the LNA IM3 tones do impact on the output IM3 tones. For simplicity the LO term is removed along with the RF term leaving only the difference terms. Therefore ω_1 = RF1-LO and ω_2 =RF2-LO.

$$V_i = cos(\omega_1 t) + cos(\omega_2 t) + Ccos\big((2\omega_1 - \omega_2)t\big) + Ccos((2\omega_2 - \omega_1)t) \qquad (18)$$

$$V_{IF} = cos(\omega_1 t)\left[\frac{9k_3}{4}(2C^2 + C + 1) + k_1\right] + cos(\omega_2 t)\left[\frac{9k_3}{4}(2C^2 + C + 1) + k_1\right]$$
$$+ cos(2\omega_1 t)\left[k_2\left(\frac{1}{2} + C\right)\right] + cos(2\omega_2 t)\left[k_2\left(\frac{1}{2} + C\right)\right]$$
$$+ cos\big((\omega_2 - \omega_1)t\big)[k_2(2C + 1)] + cos((\omega_1 + \omega_2)t)[k_2(C^2 + 1)]$$
$$+ cos(3\omega_1 t)\left[\frac{k_3}{4}(3C^3 + 6C + 1)\right] + cos(3\omega_2 t)\left[\frac{k_3}{4}(3C^3 + 6C + 1)\right]$$
$$+ cos\big((2\omega_1 + \omega_2)t\big)\left[\frac{3k_3}{4}(2C^3 + C + 1)\right] + cos((2\omega_2 + \omega_1)t)\left[\frac{3k_3}{4}(2C^3 + C + 1)\right]$$
$$+ cos\big((\omega_2 - 2\omega_1)t\big)\left[\frac{3k_3}{4}(3C^3 + 6C + 1) + k_1 C\right] + cos((2\omega_2 - \omega_1)t)\left[\frac{3k_3}{4}(3C^3 + 6C + 1) + k_1 C\right] + \ldots \qquad (19)$$

The contribution of these additional tones introduces imbalance into the system where the ω1± ω2 tones are either 2C+1 or C^2+1 which will add to system complexity if trying to null out the effect. This means that in a highly integrated receiver, containing both amplifier and mixing elements, it is a requirement to consider all tones cascading down from preceding elements.

These equations imply that the subtractive IM3 terms should always be equal being $\left[\frac{3k_3}{4}(3C^3 + 6C + 1) + k_1C\right]$ however this is almost always never the case (similar but not the same). This asymmetry is due to the presence of a reactance element on the terminating impedance [26, 27].

Using this four tone input and applying it to a perfectly balanced system, the Volterra expansion will only contain odd order products, albeit eighty six terms if expanding to the fifth order. Introducing phase error into the mix (as no circuit is ever perfect) this length increases to one hundred and sixty terms (accounting for both positive and negative phase shifts due to even and odd order multiplication) and is difficult to correlate back to the root cause of imbalance.

6. Measurement in Practice

To measure a device, two frequencies are required that are relatively close to each other in the pass band of the DUT. It is common to use a tone spacing of 10 MHz for signals greater than 1 GHz, however it is worth noting that a lot of commercial equipment uses 10 MHz reference signals which can obscure the result, so it is recommended to move to another spacing such as 11 MHz to avoid this possible issue [28]. This is particularly important for direct down conversion measurements where all the measurement tones are close to DC. The requirements for measurements are as follows:

- The two signal generators and spectrum analyser (a power meter cannot be used as they are not measuring a discrete tone level) should be locked to a reference signal for accurate measurements.
- The spectrum analyser should be set such that the resolution bandwidth can clearly resolve each tone of interest.
- The input tones should be as clean as possible, so to minimise the spurious mixing caused by the two signal generators isolators/circulators should be used. Otherwise intermodulation performance may be due to generator mixing rather than the device under test.

A schematic is shown below (Figure 9) of the final test setup for measuring intermodulation tones.

It should be also noted that there may be multiple ways to generate a single tone. That is, that higher order products may be also contributing to a signal output frequency. If

this is suspected to be the case, varying the input tone spacing will move the tones and enable the strongest interferer to be identified.

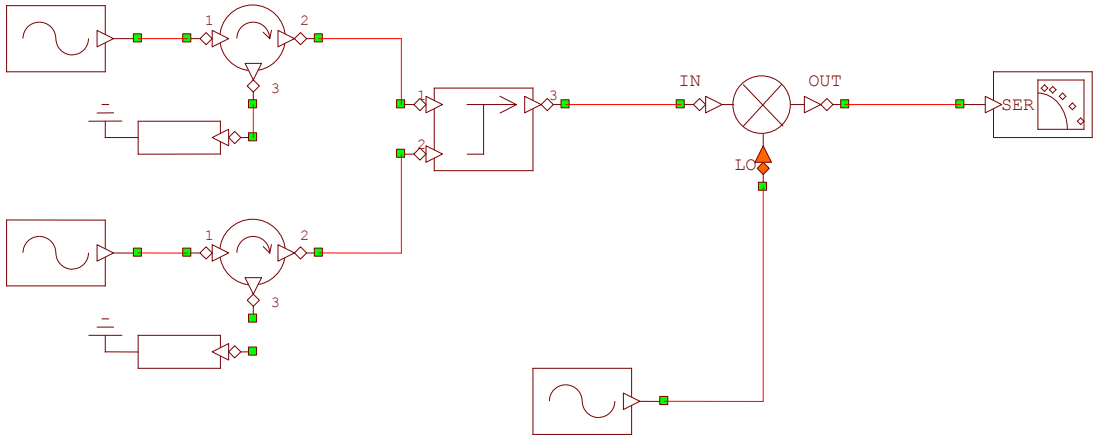

Figure 9 - Measurement Setup

The measurements below were completed with an integrated downconverter chip. The device in question is shown below. It was an engineering sample of a plastic Quad Flat No-leads (QFN) package from Macom (www.macom.com). The die is a Gallium Arsenide design based on a 0.15 µm pHEMT process at WIN Semiconductors. The on-chip LNA is a single-ended design, comprising of three stages, however stages two and three are internally tied together. The design was chosen to maximise linearity of the amplifier. The LO multiplier is operated as a frequency doubler. It consists of a pre amp, doubling stage and a post amplifier. The mixer design has four resistive Field-Effect Transistor (FET) mixers which combine to create two image reject mixers. These are combined with a Marchand balun to complete the circuit. Figure 10 shows the circuit.

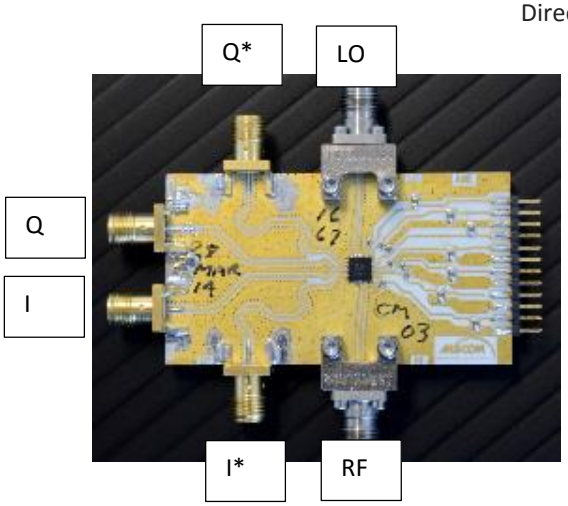

Figure 10 - GaAs Receiver

It can be seen in Figure 11 that the device operates in a linear fashion for input powers below -20 dBm. Once this power is exceeded, the system no longer operates at a linear point, which corresponds with the Taylor series expansion no longer being a valid. It has been noted that some of the intermodulation tones are not the same as predicted, indicating that there is a possibility of influence from third order tones from the LNA, and also imbalance within the mixers contributing to the final result (See Table 1).

Measurements were recorded with automated lab software written in NI LabView. This is pre-existing software written by Macom employees.

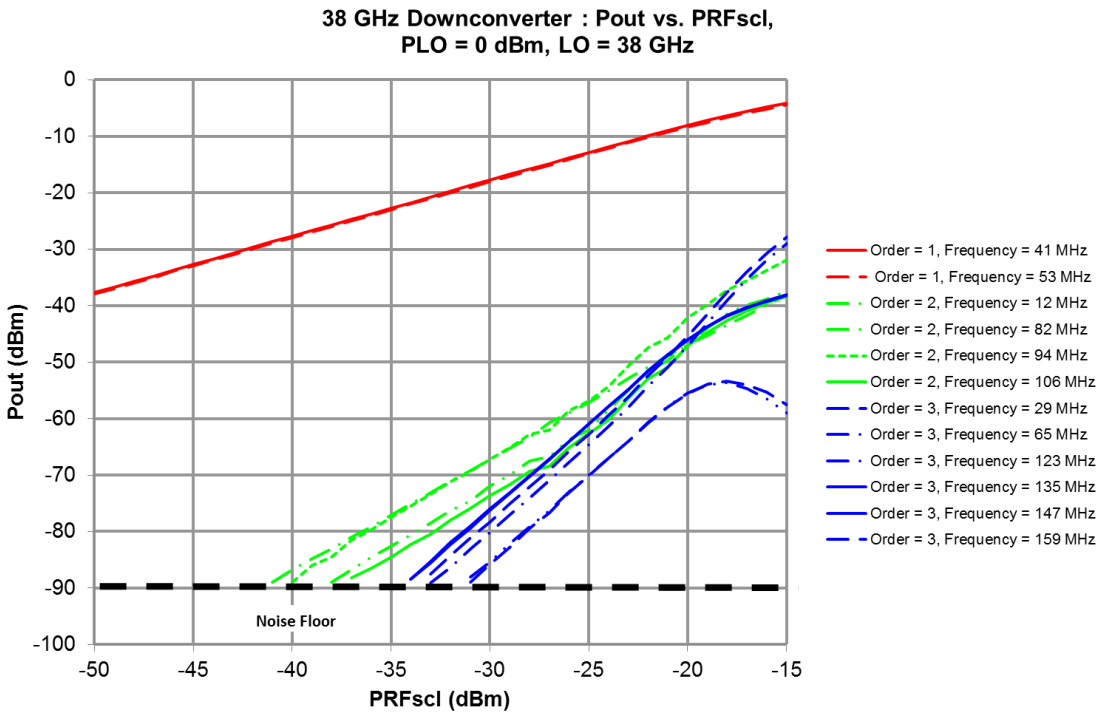

Figure 11 - Intermodulation Output Power

Figure 12 shows all terms to the seventh order. Many of these terms have already reached a compressed point before they are above the noise floor so it is difficult to extrapolate any linear dependence from these traces.

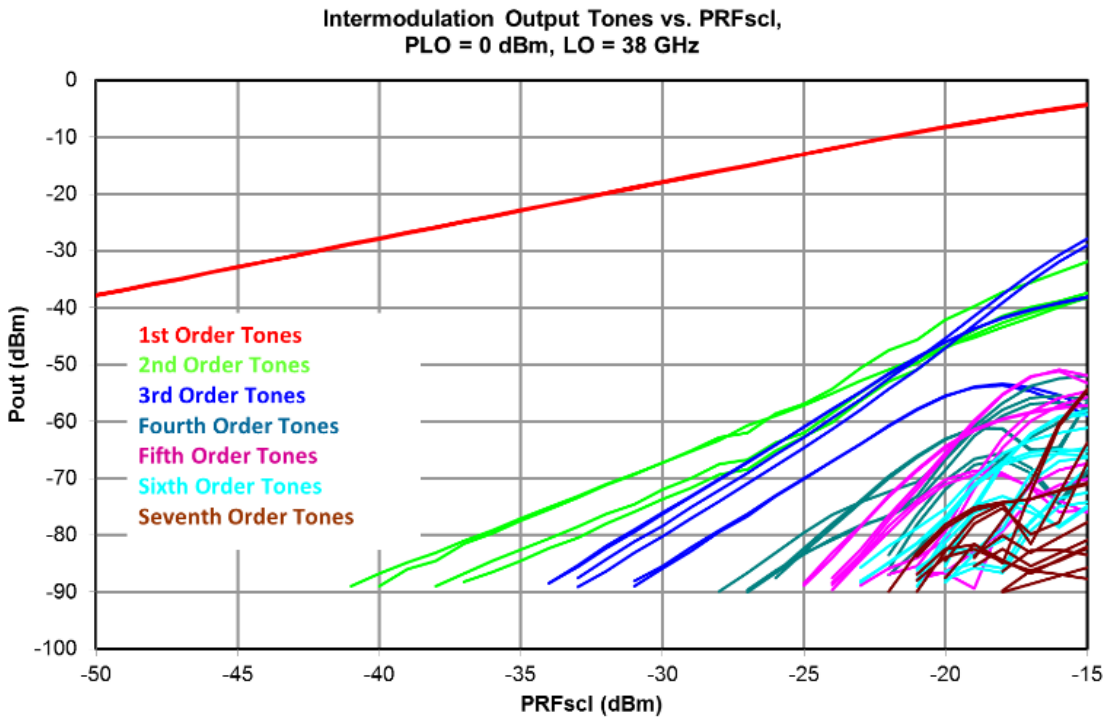

Figure 12 - Tones up to Seventh Order

A mixer cell was also fabricated. This removed the LO multiplier and LNA circuitry and enabled probing directly around the mixer (Figure 13 below shows a photo of setup with four IF outputs, one LO input and one RF input. The south side has DC cabling.). By measuring this it is possible to see in Figure 14 the distortion based on the mixer alone. In this scenario, the harmonic tones are roughly equal (as predicted) and the additive and subtractive tones are different. It can also be observed that the in this case the mixer isn't yet being driven hard enough to start compressing the wanted tones. This mixer cell was measured on bare die with probes.

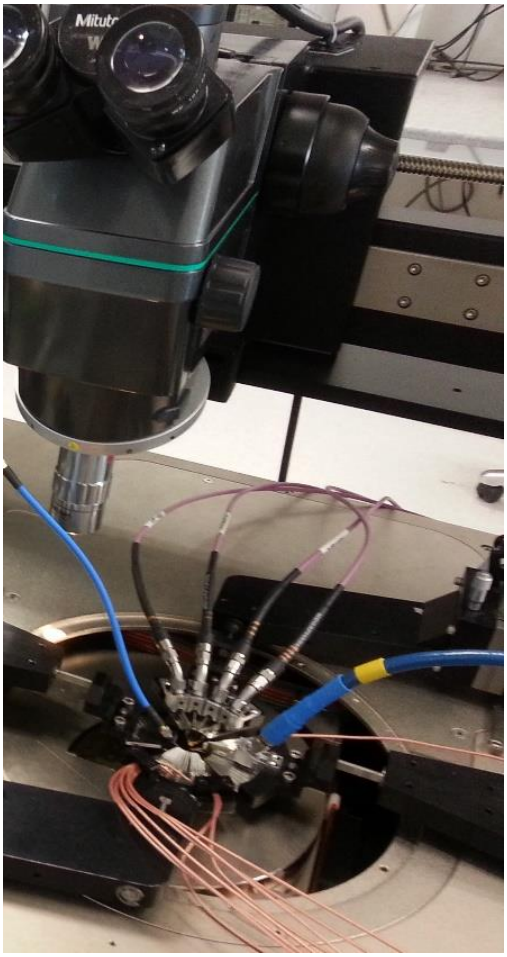

Figure 13 - Bare Die setup

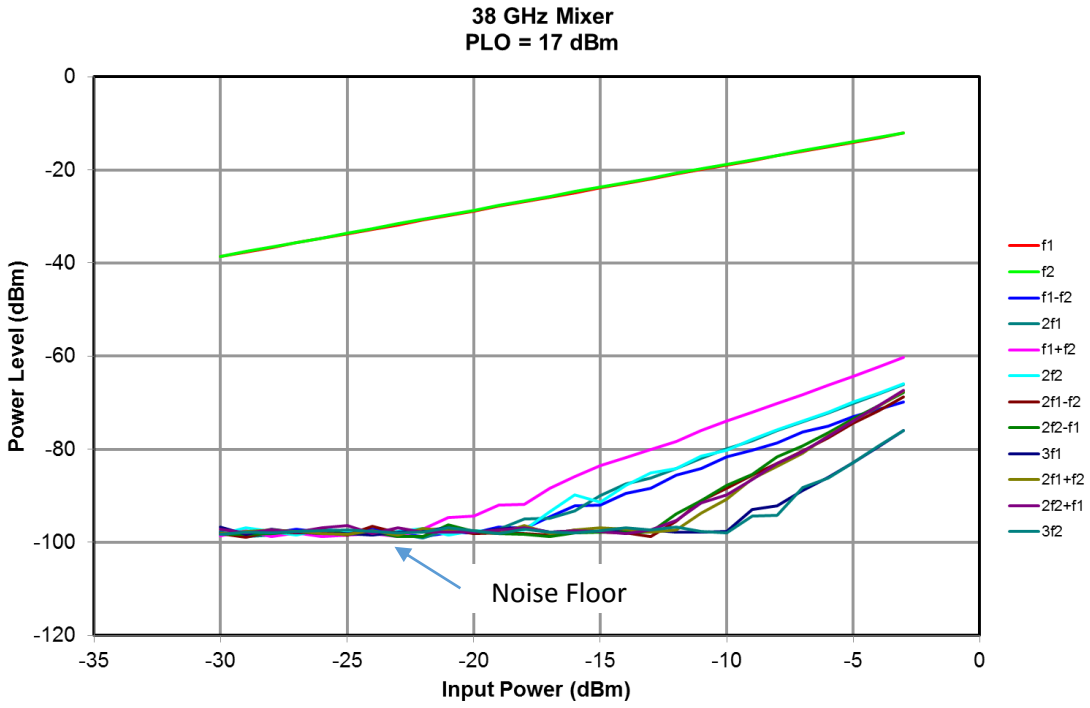

Figure 14 - Intermodulation in Mixer

The graph above shows that the tones are behaving as predicted.

That is, the first order tones ω_1, ω_2 have the same $(k_1 + \frac{9k_3}{4})$ amplitude, and the $2\omega_1, 2\omega_2$ tones have the same $(\frac{k_2}{2} + 2k_4)$ amplitude. Since the $\omega_1 + \omega_2$ and $\omega_1 - \omega_2$ tones are present it indicates imbalance in the mixer and the amount can then be estimated along with the coefficients using nonlinear solver techniques.

The GaAs based receiver incorporates a rat race coupler (Figure 15). This device splits an incoming signal two ways and also provide a 180° phase shift in one branch. When comparing different processes it is important to consider the approach of simulation of this coupler, as the IM2 results are strongly influenced by this phase difference (Figure 7). The rat race in GaAs has excellent simulated performance (Figure 16) with a phase difference of less than one degree, however the measured IM2 level is at best 40 dBc corresponding to a 5° error in phase. There is of course additional circuitry beyond the coupler that can load each branch differently, altering the phase imbalance, but it is clearly observed that balance alone from the coupler will not be the sole provider for cancellation of the IM2 components.

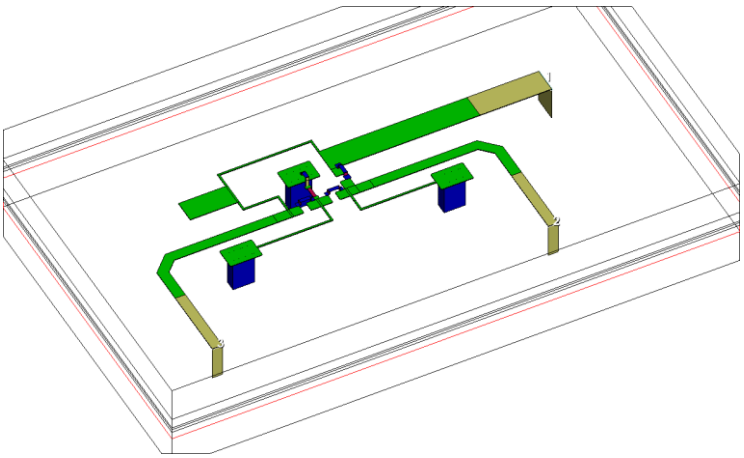

Figure 15 - Rat Race Coupler (3D Simulation)

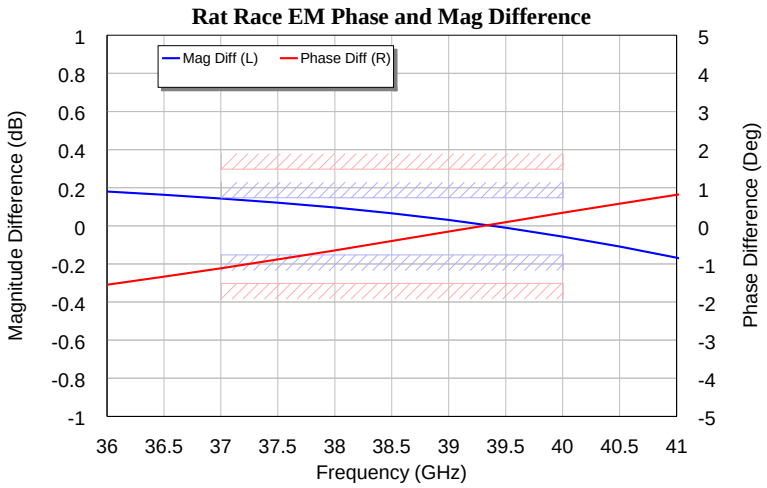

Figure 16 - Simulated Rat Race Performance

With this in mind it is quite difficult to give a clear comparison of the performance of two receivers based on two different processes and modelling techniques. Taking into account the short comings of such an analysis, we will proceed carefully with a comparison.

Two 38 GHz downconverter devices are compared from two different processes [22]. The first chip has already been described and shown in Figure 10 while the second chip is a Silicon Germanium Heterojunction Bipolar Transistor (HBT) design based on the IHP SG25H1 process in Germany (Figure 17). This is a 0.25 µm Bipolar Complementary metal-oxide semiconductor (BiCMOS) process. The architecture of this design contains a cascode LNA, Gilbert cell mixer and an LO tripler.

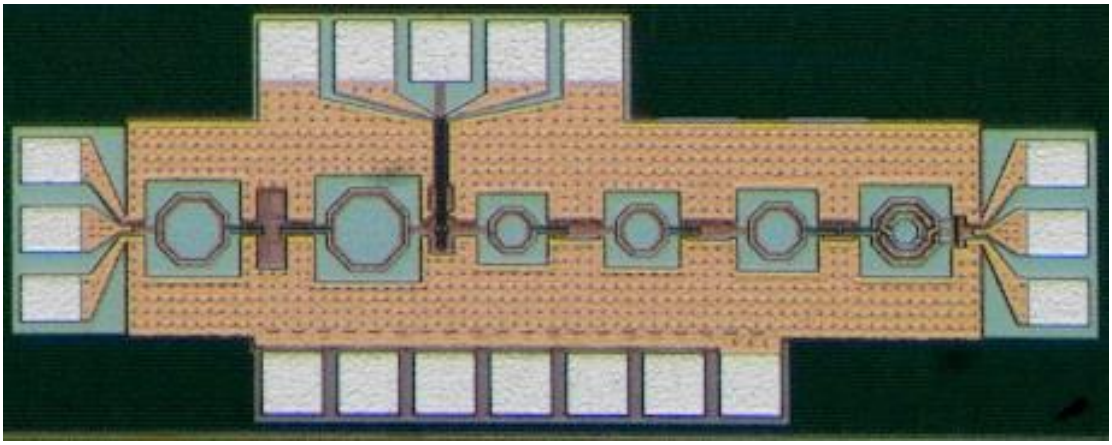

Figure 17 - SiGe Receiver

Figure 18 shows the performance of both receivers. It indicates that SiGe is better performing for even order intermod products but for the odd terms GaAs is significantly better. It is interesting to note that the inphase and quadrature channels for GaAs are not equal. In this particular case there will be a phase shift from the 180° split, generating a 0° and a 180° signal. These two signals are then split again creating I (0°) and Q (90°) and then I* (180°) and Q* (270°). None of these are perfect splits and each will introduce a level of error. Table 1 shows the deltas between I and Q measurements. It is interesting to see that the second order terms have a negative delta compared to the third order terms.

Frequency (MHz)	Order	Delta (dB)
12	2	-6.96499
82	2	-2.81099
94	2	-3.97399
106	2	-4.23699
29	3	2.351014
65	3	1.576014
123	3	5.206014
135	3	5.770014
147	3	6.615014
159	3	7.504014

Table 1 - GaAs Delta between I and Q

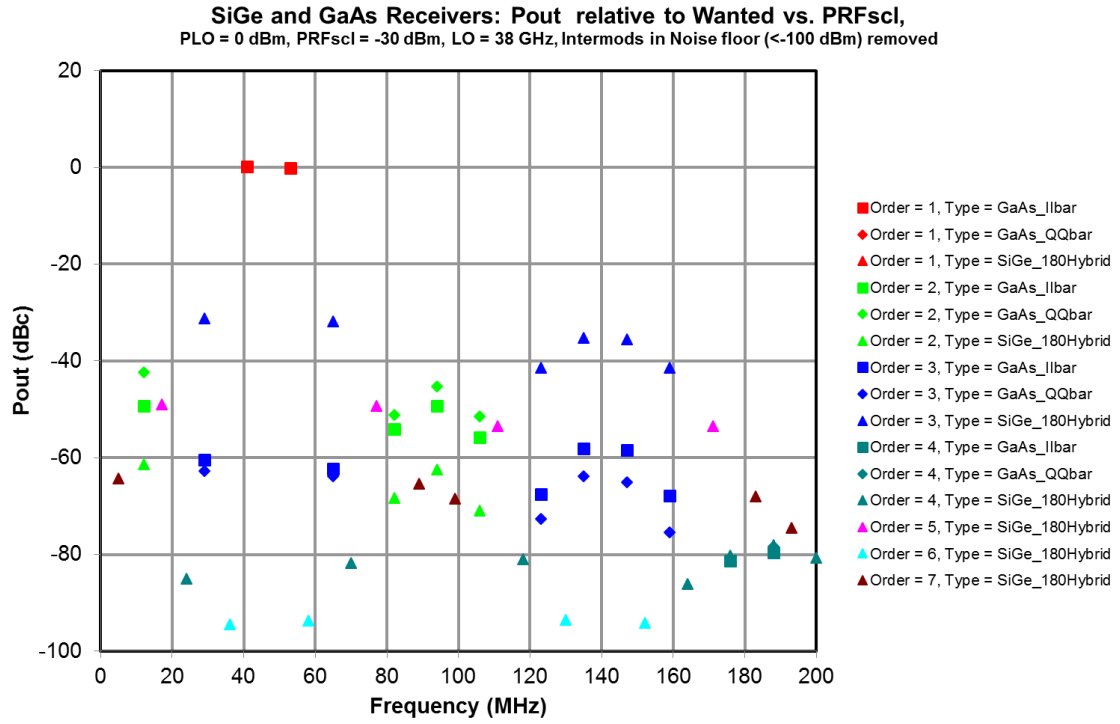

Figure 18 - GaAs and SiGe Performance

To explain the GaAs differences consider a four input feed (two wanted and two third order tones) into a 180° degree hybrid, and then an additional two 90° hybrids. This will then provide the 0, 90, 180 and 270 degree phases. Assume "a" is the phase error on 0 degree, "b" is the phase error on 180 degree, "e" is the phase error on 90 degree and "g" is the phase error on 270 degree, one obtains the following signals before the Volterra expansion.

$$0\ Degree = ACos[a + tw1] + CCos[a + t(2w1 - w2)] + ACos[a + tw2] + CCos[a + t(-w1 + 2w2)] \quad (20)$$

$$180\ Degree = -ACos[b + tw1] - ACos[b + t(2w1 - w2)] - ACos[b + tw2] - ACos[b + t(-w1 + 2w2)] \quad (21)$$

$$90\ Degree = -ASin[f + tw1] - CSin[f + t(2w1 - w2)] - ASin[f + tw2] - CSin[f + t(-w1 + 2w2)] \quad (22)$$

$$270\ Degree = A\mathrm{Sin}[g + t\mathrm{w1}] + A\mathrm{Sin}[g + t(2\mathrm{w1} - \mathrm{w2})] + A\mathrm{Sin}[g + t\mathrm{w2}] + A\mathrm{Sin}[g + t(-\mathrm{w1} + 2\mathrm{w2})] \quad (23)$$

Frequency	Order	I (0+180 degree)	Q (90 + 270 degree)
12	2	$(-2A^2\text{k2} + 2AC\text{k2} - 27A^4\text{k4} + 9A^3C\text{k4} + 9A^2C^2\text{k4} + 9AC^3\text{k4})\text{Cos}[12t]$	$(-2A^2\text{k2} + 2AC\text{k2} - 27A^4\text{k4} + 9A^3C\text{k4} + 9A^2C^2\text{k4} + 9AC^3\text{k4})\text{Cos}[12t]$
82	2	$(\frac{A^2\text{k2}}{2} + AC\text{k2} + 2A^4\text{k4} + 6A^3C\text{k4} + 6A^2C^2\text{k4} + 6AC^3\text{k4})\text{Cos}[2a + 82t] + (-\frac{3A^2\text{k2}}{2} - 20A^4\text{k4})\text{Cos}[2b + 82t]$	$(-\frac{A^2\text{k2}}{2} - AC\text{k2} - 2A^4\text{k4} - 6A^3C\text{k4} - 6A^2C^2\text{k4} - 6AC^3\text{k4})\text{Cos}[2f + 82t] + (\frac{3A^2\text{k2}}{2} + 20A^4\text{k4})\text{Cos}[2g + 82t]$
94	2	$(A^2\text{k2} + C^2\text{k2} + 3A^4\text{k4} + 4A^3C\text{k4} + 12A^2C^2\text{k4} + 3C^4\text{k4})\text{Cos}[2a + 94t] + (-2A^2\text{k2} - 22A^4\text{k4})\text{Cos}[2b + 94t]$	$(-A^2\text{k2} - C^2\text{k2} - 3A^4\text{k4} - 4A^3C\text{k4} - 12A^2C^2\text{k4} - 3C^4\text{k4})\text{Cos}[2f + 94t] + (2A^2\text{k2} + 22A^4\text{k4})\text{Cos}[2g + 94t]$
106	2	$(\frac{A^2\text{k2}}{2} + AC\text{k2} + 2A^4\text{k4} + 6A^3C\text{k4} + 6A^2C^2\text{k4} + 6AC^3\text{k4})\text{Cos}[2a + 106t] + (-\frac{3A^2\text{k2}}{2} - 20A^4\text{k4})\text{Cos}[2b + 106t]$	$(-\frac{A^2\text{k2}}{2} - AC\text{k2} - 2A^4\text{k4} - 6A^3C\text{k4} - 6A^2C^2\text{k4} - 6AC^3\text{k4})\text{Cos}[2f + 106t] + (\frac{3A^2\text{k2}}{2} + 20A^4\text{k4})\text{Cos}[2g + 106t]$
29	3	$(C\text{k1} + \frac{3A^3\text{k3}}{4} + \frac{9}{2}A^2C\text{k3} + \frac{9C^3\text{k3}}{4} + \frac{25A^5\text{k5}}{8} + \frac{75}{4}A^4C\text{k5} + \frac{75}{4}A^3C^2\text{k5} + \frac{75}{2}A^2C^3\text{k5} + \frac{25C^5\text{k5}}{4})\text{Cos}[a + 29t] + (A\text{k1} + \frac{15A^3\text{k3}}{2} + \frac{675A^5\text{k5}}{8})\text{Cos}[b + 29t]$	$(-C\text{k1} - \frac{3A^3\text{k3}}{4} - \frac{9}{2}A^2C\text{k3} - \frac{9C^3\text{k3}}{4} - \frac{25A^5\text{k5}}{8} - \frac{75}{4}A^4C\text{k5} - \frac{75}{4}A^3C^2\text{k5} - \frac{75}{2}A^2C^3\text{k5} - \frac{25C^5\text{k5}}{4})\text{Sin}[f + 29t] + (-A\text{k1} - \frac{15A^3\text{k3}}{2} - \frac{675A^5\text{k5}}{8})\text{Sin}[g + 29t]$
65	3	$(C\text{k1} + \frac{3A^3\text{k3}}{4} + \frac{9}{2}A^2C\text{k3} + \frac{9C^3\text{k3}}{4} + \frac{25A^5\text{k5}}{8} + \frac{75}{4}A^4C\text{k5} + \frac{75}{4}A^3C^2\text{k5} + \frac{75}{2}A^2C^3\text{k5} + \frac{25C^5\text{k5}}{4})\text{Cos}[a + 65t] + (A\text{k1} + \frac{15A^3\text{k3}}{2} + \frac{675A^5\text{k5}}{8})\text{Cos}[b + 65t]$	$(-C\text{k1} - \frac{3A^3\text{k3}}{4} - \frac{9}{2}A^2C\text{k3} - \frac{9C^3\text{k3}}{4} - \frac{25A^5\text{k5}}{8} - \frac{75}{4}A^4C\text{k5} - \frac{75}{4}A^3C^2\text{k5} - \frac{75}{2}A^2C^3\text{k5} - \frac{25C^5\text{k5}}{4})\text{Sin}[f + 65t] + (-A\text{k1} - \frac{15A^3\text{k3}}{2} - \frac{675A^5\text{k5}}{8})\text{Sin}[g + 65t]$
123	3	$(\frac{A^3\text{k3}}{4} + \frac{3}{2}A^2C\text{k3} + \frac{3C^3\text{k3}}{4} + \frac{25A^5\text{k5}}{16} + \frac{75}{8}A^4C\text{k5} + \frac{75}{8}A^3C^2\text{k5} + \frac{75}{4}A^2C^3\text{k5} + \frac{25C^5\text{k5}}{8})\text{Cos}[3a + 123t] + (\frac{5A^3\text{k3}}{2} + \frac{675A^5\text{k5}}{16})\text{Cos}[3b + 123t]$	$(\frac{A^3\text{k3}}{4} + \frac{3}{2}A^2C\text{k3} + \frac{3C^3\text{k3}}{4} + \frac{25A^5\text{k5}}{16} + \frac{75}{8}A^4C\text{k5} + \frac{75}{8}A^3C^2\text{k5} + \frac{75}{4}A^2C^3\text{k5} + \frac{25C^5\text{k5}}{8})\text{Sin}[3f + 123t] + (\frac{5A^3\text{k3}}{2} + \frac{675A^5\text{k5}}{16})\text{Sin}[3g + 123t]$
135	3	$(\frac{3A^3\text{k3}}{4} + \frac{3}{4}A^2C\text{k3} + \frac{3}{2}AC^2\text{k3} + \frac{25A^5\text{k5}}{8} + \frac{125}{16}A^4C\text{k5} + \frac{75}{4}A^3C^2\text{k5} + \frac{75}{8}A^2C^3\text{k5} + \frac{75}{8}AC^4\text{k5})\text{Cos}[3a + 135t] + (3A^3\text{k3} + \frac{775A^5\text{k5}}{16})\text{Cos}[3b + 135t]$	$(\frac{3A^3\text{k3}}{4} + \frac{3}{4}A^2C\text{k3} + \frac{3}{2}AC^2\text{k3} + \frac{25A^5\text{k5}}{8} + \frac{125}{16}A^4C\text{k5} + \frac{75}{4}A^3C^2\text{k5} + \frac{75}{8}A^2C^3\text{k5} + \frac{75}{8}AC^4\text{k5})\text{Sin}[3f + 135t] + (3A^3\text{k3} + \frac{775A^5\text{k5}}{16})\text{Sin}[3g + 135t]$
147	3	$(\frac{3A^3\text{k3}}{4} + \frac{3}{4}A^2C\text{k3} + \frac{3}{2}AC^2\text{k3} + \frac{25A^5\text{k5}}{8} + \frac{125}{16}A^4C\text{k5} + \frac{75}{4}A^3C^2\text{k5} + \frac{75}{8}A^2C^3\text{k5} + \frac{75}{8}AC^4\text{k5})\text{Cos}[3a + 147t] + (3A^3\text{k3} + \frac{775A^5\text{k5}}{16})\text{Cos}[3b + 147t]$	$(\frac{3A^3\text{k3}}{4} + \frac{3}{4}A^2C\text{k3} + \frac{3}{2}AC^2\text{k3} + \frac{25A^5\text{k5}}{8} + \frac{125}{16}A^4C\text{k5} + \frac{75}{4}A^3C^2\text{k5} + \frac{75}{8}A^2C^3\text{k5} + \frac{75}{8}AC^4\text{k5})\text{Sin}[3f + 147t] + (3A^3\text{k3} + \frac{775A^5\text{k5}}{16})\text{Sin}[3g + 147t]$
159	3	$(\frac{A^3\text{k3}}{4} + \frac{3}{2}A^2C\text{k3} + \frac{3C^3\text{k3}}{4} + \frac{25A^5\text{k5}}{16} + \frac{75}{8}A^4C\text{k5} + \frac{75}{8}A^3C^2\text{k5} + \frac{75}{4}A^2C^3\text{k5} + \frac{25C^5\text{k5}}{8})\text{Cos}[3a + 159t] + (\frac{5A^3\text{k3}}{2} + \frac{675A^5\text{k5}}{16})\text{Cos}[3b + 159t]$	$(\frac{A^3\text{k3}}{4} + \frac{3}{2}A^2C\text{k3} + \frac{3C^3\text{k3}}{4} + \frac{25A^5\text{k5}}{16} + \frac{75}{8}A^4C\text{k5} + \frac{75}{8}A^3C^2\text{k5} + \frac{75}{4}A^2C^3\text{k5} + \frac{25C^5\text{k5}}{8})\text{Sin}[3f + 159t] + (\frac{5A^3\text{k3}}{2} + \frac{675A^5\text{k5}}{16})\text{Sin}[3g + 159t]$

Table 2 - I & Q Order

Revisiting Table 1 it can be noted that from the third order tones, the 29 and 65 MHz deltas are distinct from the other four third order tones. This can be attributed to

some degree by the single order phase error, whereas the other four terms all require the phase error be multiplied by three. Also, the even order tones are all inphase (hence why balance generally will cancel out terms) whereas the odd tones are distinctly cosine and sine waves and hence in quadrature.

Does this mean that in general IM2 is better with SiGe than GaAs? Not quite. A single ended amplifier may show this, but for these devices with multiple functions, it tends to indicate that the balance of the 180° split over the entire MMIC is better with SiGe.

Efforts to compute the phase error based on equations such as (17) so far have not returned accurate results. It would be more effective to use a four channel ADC that can capture up to 300 MHz of bandwidth, then manually compute both the phase and amplitude of each tone, and mathematically work out how much phase change is required. Alternatively, analogue phase shifters could be used. At 12 MHz the wavelength is 25 metres which would require quite a large track length to change the phase. A circuit like Minicircuits JSPHS-12+ [29] would also enable visibility on a spectrum analyser to see what phase shift would be required.

Referring back to equation (19), we can now compare the output of the measured tones with respect to what was calculated. Figure 19 shows that the predicted coefficients correlate to the measured data (for example $2f_1$ and $2f_2$ have equal powers of $k_2\left(\frac{1}{2}+C\right)$ and this is seen in measured data). The SiGe tones are slightly unbalanced but this is due to SiGe device starting to compress at this "slice" of data. Figure 20 then examines the third order tones. Again the predicted expansion matches the measured results quite well, indicating that when considering the expansion of the integrated

device, the individual parts need to be considered otherwise the expansion does not compute.

Comparisons at higher orders cannot be made with current data as either the GaAs parts are below the noise floor or the SiGe parts are undergoing too much compression.

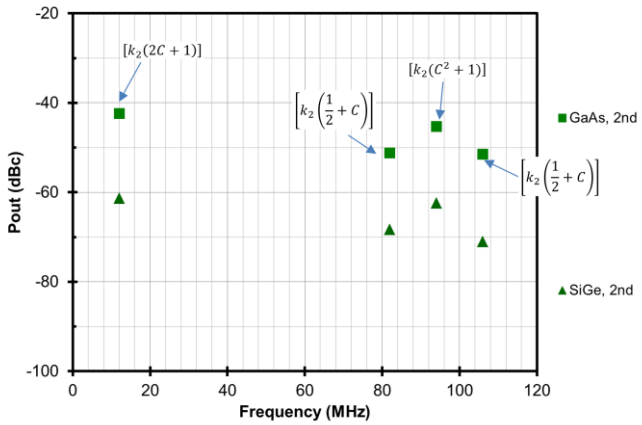

Figure 19 - Second Order Results

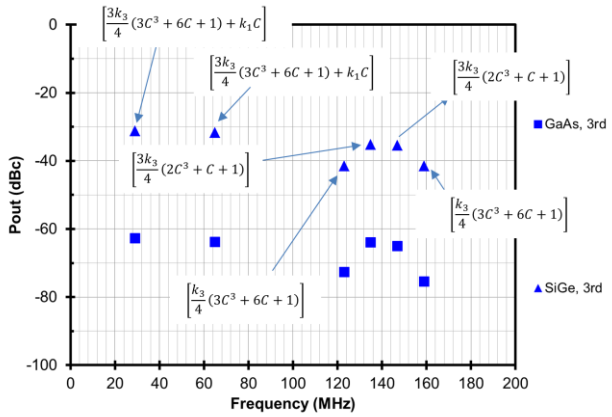

Figure 20 - Third Order Results

There is also a relationship between the LO signal and the intermodulation performance. That is, by varying the input LO power it is possible to find power levels that improve the intermodulation performance of the device while maintaining the gain. Contour graphs shown below in Table 3 show a number of tones varying both input and LO power (white regions indicate noise floor defined as -100 dBm). It can be seen

it is possible to improve the intercept point of one frequency it doesn't necessarily mean that it will improve the other points even within the same order. For instance with SiGe the 12 MHz tone exhibits two optimal points, the first around -35 dBm input power and 3 dBm LO and the second with -19 dBm input power and 0 dBm LO. This second peak is misleading as the device is well compressed at this point and therefore, this won't be an optimal point in general for operation.

This method of representing both output power and IPn gives a great deal of insight into the operation of the device. The first graphs (plotting output power) show that the GaAs part is not dependant on LO power (over the -6 to +6 dBm range) as each decibel of input power results in a linear increase in output power. Conversely the SiGe part at the lower end of the scale shows that the LO drive into the mixer isn't sufficient at lower power levels. Secondly the linear spacing of output power isn't consistent, showing that at the higher power levels the device is starting to compress and no longer can increase in output power. Overall the GaAs parts have a much more even distribution i.e. that there isn't much variability of performance over differing power levels with multiple tones compared to the SiGe part. This reflects a difference in architecture moreso than limitations of either process.

Table 3 - IIPn Contour Graphs for different tones (GaAs left & SiGe right)

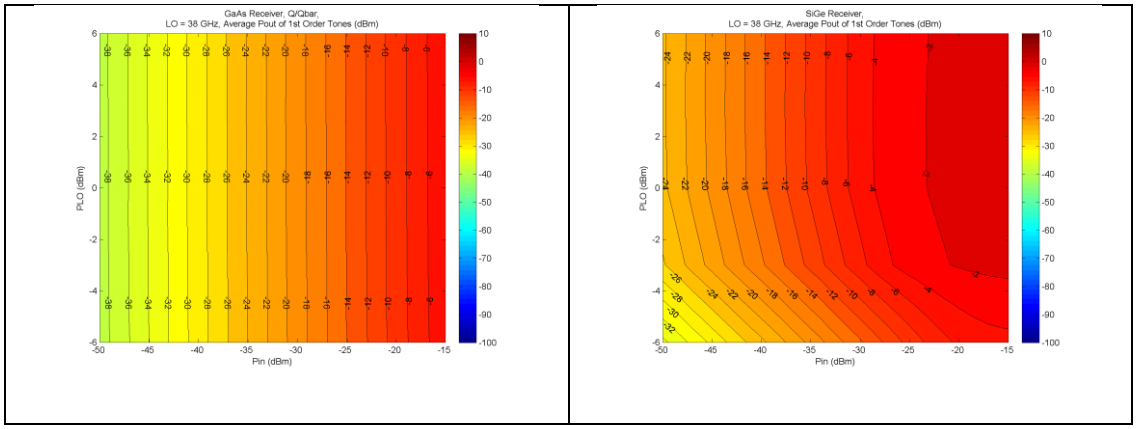

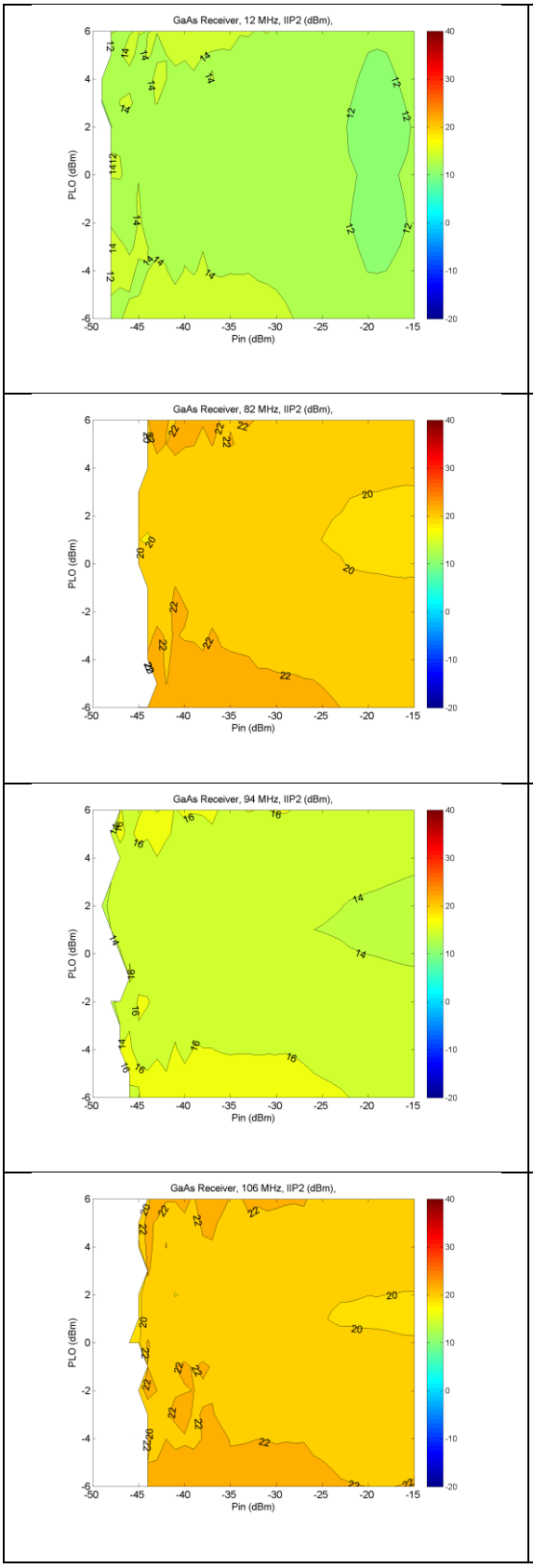
GaAs Receiver, 12 MHz, IIP2 (dBm),
SiGe Receiver, 12 MHz, IIP2 (dBm),
GaAs Receiver, 82 MHz, IIP2 (dBm),
SiGe Receiver, 82 MHz, IIP2 (dBm),
GaAs Receiver, 94 MHz, IIP2 (dBm),
SiGe Receiver, 94 MHz, IIP2 (dBm),
GaAs Receiver, 106 MHz, IIP2 (dBm),
SiGe Receiver, 106 MHz, IIP2 (dBm),
PLO (dBm)
Pin (dBm)

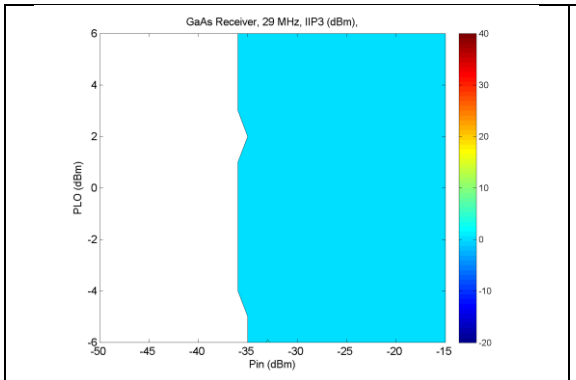
GaAs Receiver, 29 MHz, IIP3 (dBm),
PLO (dBm)
Pin (dBm)

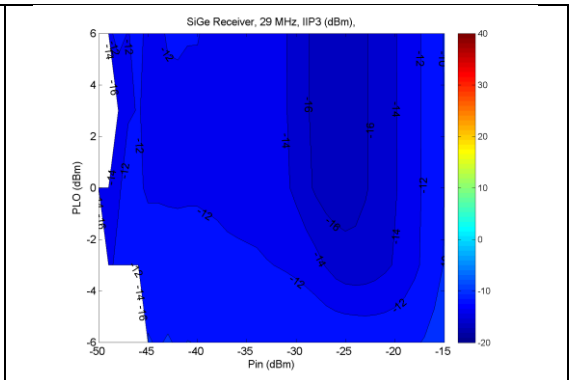
SiGe Receiver, 29 MHz, IIP3 (dBm),
PLO (dBm)
Pin (dBm)

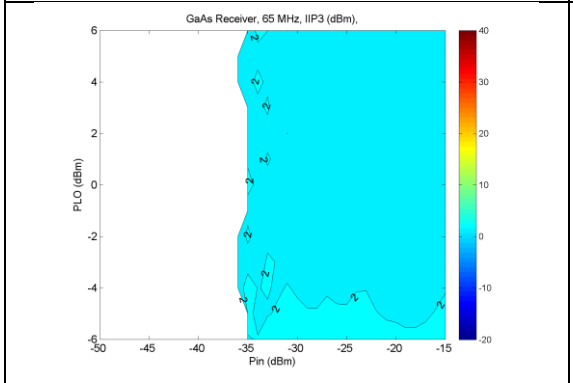
GaAs Receiver, 65 MHz, IIP3 (dBm),
PLO (dBm)
Pin (dBm)

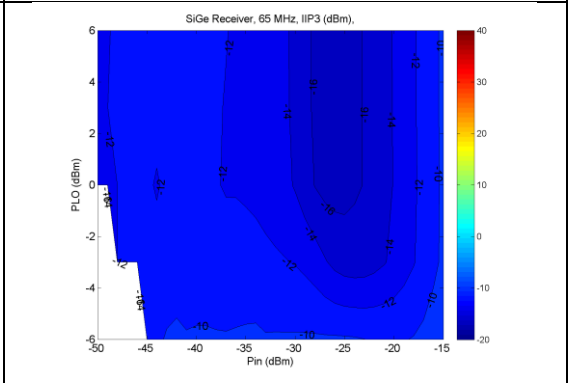
SiGe Receiver, 65 MHz, IIP3 (dBm),
PLO (dBm)
Pin (dBm)

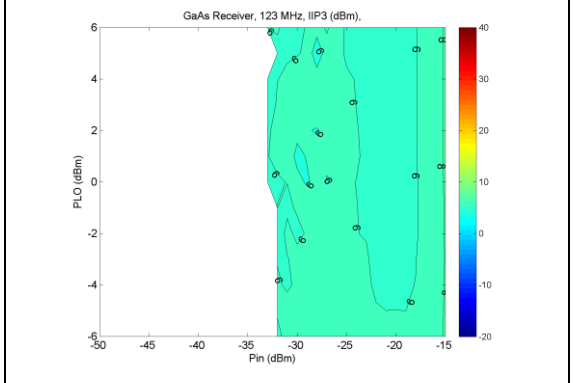
GaAs Receiver, 123 MHz, IIP3 (dBm),
PLO (dBm)
Pin (dBm)

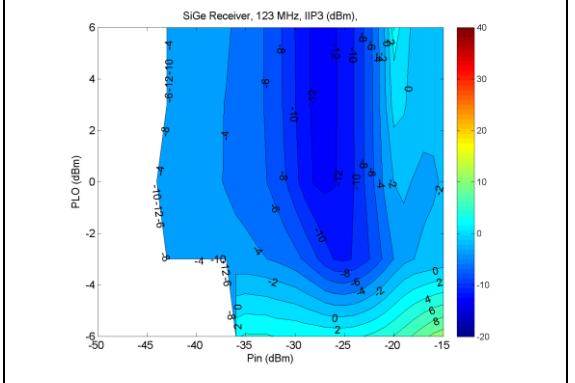
SiGe Receiver, 123 MHz, IIP3 (dBm),
PLO (dBm)
Pin (dBm)

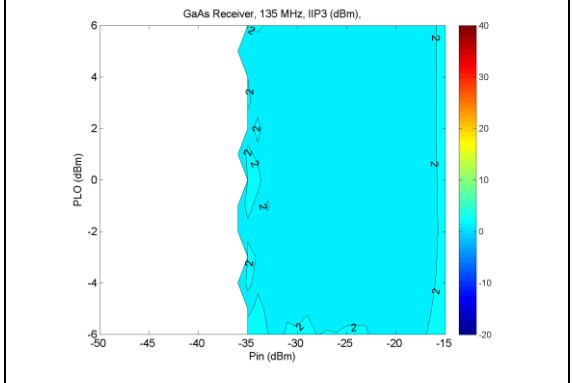
GaAs Receiver, 135 MHz, IIP3 (dBm),
PLO (dBm)
Pin (dBm)

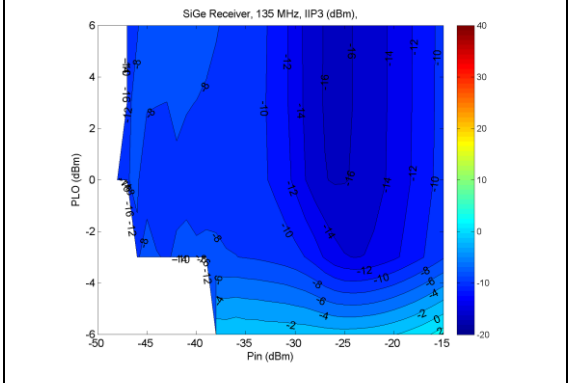
SiGe Receiver, 135 MHz, IIP3 (dBm),
PLO (dBm)
Pin (dBm)

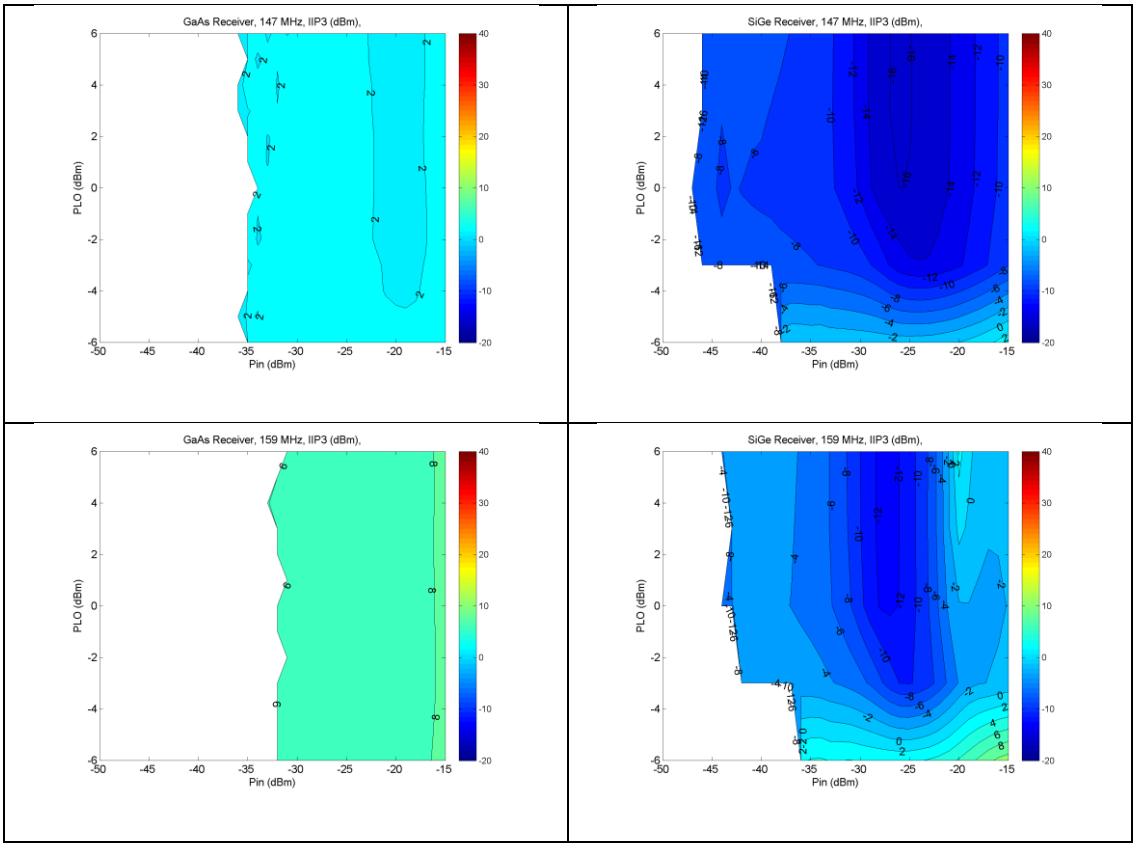
GaAs Receiver, 147 MHz, IIP3 (dBm),
SiGe Receiver, 147 MHz, IIP3 (dBm),
GaAs Receiver, 159 MHz, IIP3 (dBm),
SiGe Receiver, 159 MHz, IIP3 (dBm),
PLO (dBm)
Pin (dBm)

7. Conclusion

Direct down conversion receiver architectures were reviewed, and in particular intermodulation performance and resultant balance challenges were discussed. Two 38 GHz receivers based on different architectures and processes were measured and compared. The GaAs receiver tended to have significantly better odd order performance while the SiGe part had better even order (IM2) performance. The higher order even order terms were influenced by compression so limited conclusions can be drawn from this data. In a perfectly balanced system, even order performance should be similar (they should cancel each other out) but in real world measurements differences still exist, indicating neither has attained perfect balance.

The analysis is complicated by the differing amplifier and mixer gains in the two devices making normalisation a challenge. Further work is planned to arrive at a more concrete comparison between differing semiconductor processes in terms of noise, linearity and power consumption as well as normalised cost for production and prototype die as a function of market volume.

8. References

1. *HOMODYNE AND SYNCHRODYNE*. [cited 2015; Available from: http://www.thevalvepage.com/radtech/synchro/section2/section2.htm.
2. Gao, J., J. Tang, and K. Sheng. *Study of flicker noise for zero-IF receiver*. in *Progress Electromagnetics Research Symp. Online (PIERS)*. 2005.
3. Yamaji, T., H. Tanimoto, and H. Kokatsu, *An I/Q active balanced harmonic mixer with IM2 cancelers and a 45° phase shifter.* Solid-State Circuits, IEEE Journal of, 1998. **33**(12): p. 2240-2246.
4. Rubiola, E., *Tutorial on the double balanced mixer.* arXiv preprint physics/0608211, 2006.
5. Milotti, E., *1/ f noise: a pedagogical review.* 2002.
6. HALLEY, J.M. and P. INCHAUSTI, *The increasing importance of 1/f-noises as models of ecological variability.* Fluctuation and Noise Letters, 2004. **4**(02): p. R1-R26.
7. Johnson, J., *The Schottky Effect in Low Frequency Circuits.* Physical review, 1925. **26**(1): p. 71-85.
8. Boudot, R. and E. Rubiola, *Phase noise in RF and microwave amplifiers.* IEEE Transactions on Ultrasonics, Ferroelectrics and Frequency Control, 2012. **59**(12): p. 2613-2624.
9. Hughes, B., N.G. Fernandez, and J.M. Gladstone, *GaAs FETs with a flicker- noise corner below 1 MHz.* IEEE Transactions on Electron Devices, 1987. **34**(4): p. 733-741.
10. Johnson, J.B., *Thermal agitation of electricity in conductors.* Physical review, 1928. **32**(1): p. 97.
11. Nelson, C. *Phase Noise Measurements*. 2011 [cited 2014 27/4/2014]; Amplitude and Phase Noise Tutorial: Joint IFCS / EFTF Conference]. Available from: http://www.ifcs-eftf2011.org/sites/ifcs-eftf2011.org/files/editor-files/Slides_Nelson.pdf.
12. Pavlidis, D. *HBT vs. PHEMT vs. MESFET: What's best and why*. in *International Conference on Compound Semiconductor Manufacturing Technology*. 1999.
13. Campbell, R. and T. Semiconductor, *An integrated IQ mixer for software-defined radio applications.* High Frequency Electronics, 2004. **3**(1): p. 26-33.
14. Huang, C.-e., et al., *1/f Noise Characteristics and High-Frequency Noise Performance of InGaP/InGaAs/GaAs and InGaP/InGaAs/AlGaAs PHEMTs.*
15. Manstretta, D., R. Castello, and F. Svelto, *Low 1/ f noise CMOS active mixers for direct conversion.* IEEE Transactions on Circuits and Systems II: Analog and Digital Signal Processing, 2001. **48**(9): p. 846-850.
16. Jinsung Park, J.P., et al., *Design and Analysis of Low Flicker- Noise CMOS Mixers for Direct- Conversion Receivers.* IEEE Transactions on Microwave Theory and Techniques, 2006. **54**(12): p. 4372-4380.
17. Systems, S.R., *Low Noise Voltage Preamplifier*. 2015: http://www.thinksrs.com/downloads/PDFs/Catalog/SR560c.pdf.
18. Rubiola, E., F. Lardet-vieudrin, and F. Lardet-Vieudrin, *Low flicker- noise dc amplifier for 50 Ohm sources.* 2005.
19. Barnes, C., et al. *Residual PM noise evaluation of radio frequency mixers*. in *Frequency Control and the European Frequency and Time Forum (FCS), 2011 Joint Conference of the IEEE International*. 2011. IEEE.
20. Griffith, B. *Low Noise Mixer Preamp*. 2014 27/4/2014; Available from: http://www.ko4bb.com/~bruce/LowNoiseMixerPreamp.html.
21. Hansen, M., *Achieving Accurate On-Wafter Flicker Noise Measurements through 30 MHz.* 2009.

22. Clement, R.M., et al. *Direct Down-Conversion 38 GHz GaAs and SiGe Receivers*. in *Compound Semiconductor Integrated Circuit Symposium (CSICs), 2014 IEEE*. 2014.
23. Tannir, D. and R. Khazaka. *Computation of IP3 using single-tone moments analysis*. in *Design, Automation & Test in Europe Conference & Exhibition, 2009. DATE '09.* 2009.
24. *Second and Third Order Intercept Points*. [cited 2014 29/9/2014]; Available from: http://rf-mw.org/nonlinearity_effercts_nonlinearity_effercts_second_and_third_order_intercept_points.html.
25. Cripps, S.C., *The Intercept Point Deception [Microwave Bytes].* Microwave Magazine, IEEE, 2007. **8**(1): p. 44-50.
26. Carvalho, N.B. and J.C. Pedro. *Two-tone IMD asymmetry in microwave power amplifiers*. in *Microwave Symposium Digest. 2000 IEEE MTT-S International*. 2000.
27. Brinkhoff, J. and A.E. Parker, *Effect of baseband impedance on FET intermodulation.* Microwave Theory and Techniques, IEEE Transactions on, 2003. **51**(3): p. 1045-1051.
28. Agilent *Amplifier and CW Swept Intermodulation - Distortion Measurements*. http://literature.cdn.keysight.com/litweb/pdf/5988-9474EN.pdf.
29. Minicircuits. *Datasheet: JSPHS-12*. 2015; Available from: http://www.minicircuits.com/pdfs/JSPHS-12.pdf.